Theoretical Ecology (2025) 18:2
https://doi.org/10.1007/s12080-024-00599-z

RESEARCH

Biological invasions forming intraguild predation communities in homogeneous and heterogeneous landscapes

Silas Poloni[1,2] · **Roberto André Kraenkel**[1] · **Renato Mendes Coutinho**[3]

Received: 19 August 2024 / Accepted: 14 November 2024

Abstract

Intraguild predation (IGP) allows for coexistence between two consumers of a single resource, as long as the intraguild prey (IG prey) is competitively superior to the intraguild predator (IG predator) and resource population productivity is neither abundant or limiting. Here, we explore biological invasions forming IGP community modules by either introducing IG prey or IG predator species to established consumer-resource populations in homogeneous and heterogeneous landscapes, using reaction-diffusion equations as our modeling framework. Our main methods of analysis are comparing numerical solutions to linearization techniques and homogenization approximations. We find that in homogeneous landscapes, speeds are linearly determinate, i.e., depend on low invader population densities at the leading edge. We also find traveling wave solutions and dynamical stabilization regimes. On heterogeneous landscapes, our results show that depending on habitat preferences of the three species involved, coexistence regimes can occur regardless of IG-prey being least effective consumer, or be hindered even when IG-prey remains as the dominant competitor. Our work assesses how fast can organisms invade novel landscapes in presence of a established IG prey or IG predator and also demonstrates how habitat fragmentation and species habitat preference can disrupt or facilitate coexistence in IGP communities.

Keywords Spatial ecology · Population dynamics · Reaction-diffusion equations · Mathematical models

Introduction

Often, the introduction of new consumer species in a novel habitat can generate intraguild predation (IGP) interactions (Alhmedi et al. 2010; Tuckett et al. 2021; Bampfylde and Lewis 2007), a multi-species trophic network where exploitative competitors for a shared resource present a predator–prey relation (Polis et al. 1989; Polis and Holt 1992). This may lead to exclusion of native species, failure of invasion, or the formation of an IGP community (Tuckett et al. 2021; Montserrat et al. 2012; Fritts and Rodda 1998; Grosholz and Ruiz 1995). Alongside interspecific interactions, landscape heterogeneity plays an important role on species spatial distributions, coexistence regimes, and movement behavior (Polis et al. 1997; Schtickzelle and Baguette 2003; Abrams 2007), which in turn may also significantly change how invasions occur. Because so many factors can alter the course of range expansion events, spatially structured mathematical models have been vastly used to explore possible outcomes of biological invasions, and significant advances in the field allow us to estimate spreading speeds (see, for instance, Castillo-Chavez et al. (2013)) and analyze heterogeneous landscapes in a simplified manner (see Yurk and Cobbold 2018; Cobbold et al. 2022). Nonetheless, three species IGP communities have not been studied in detail in such contexts and can reveal regime shifts caused by the invasion of novel consumers, as well as the main factors

---

Roberto André Kraenkel and Renato Mendes Coutinho are authors that contributed equally to this work.

✉ Silas Poloni
silaspoloni@uvic.ca

Roberto André Kraenkel
roberto.kraenkel@unesp.br

Renato Mendes Coutinho
renato.coutinho@ufabc.edu.br

[1] Institute of Theoretical Physics, São Paulo State University, R. Dr. Bento Teobaldo Ferraz, 271, São Paulo 01140-070, São Paulo, Brazil

[2] Department of Biology, University of Victoria, 3800, Finnerty Road, Victoria V8P 5C2, British Columbia, Canada

[3] Center for Mathematics, Computing and Cognition, Federal University of ABC, Av. dos Estados, 5001, Santo André 09210-580, São Paulo, Brazil

behind it, such as the interplay of demographic traits and dispersal behaviors (Holt and Polis 1997). In this work, we study a three-species IGP model in different landscape settings and provide spreading speeds estimates, show some of the regimes found numerically, and provide some key factors that change community formation processes.

Theoretical approaches for population spread have been continuously developed to provide qualitative and quantitative expectations of different biological and ecological processes that take place during invasions. The pioneering works of Fisher (1937); Kolmogorov et al. (1937) and Skellam (1951) helped establish reaction diffusion equations (RDE) as the main workhorses of spatial ecology. In this modeling framework, individuals of a given species are assumed to move with Brownian motion (hence diffusion), and population levels change according to the relevant biological processes governing demography, such as reproduction, death, and intra-specific competition (hence reaction). This modeling approach allows for estimates of asymptotic spreading speeds of an invasive species, which in various cases are linearly determinate, i.e., they depend on the dynamics of a low density invading population in face of an established resident community (Weinberger 1978; Lewis et al. 2002; Castillo-Chavez et al. 2013). Such models may also present traveling wave solutions, i.e., spatial profiles that are maintained through time, but advance in space, signaling the range expansion and establishment of invading species (Weinberger 1982; Hosono 1998; Lewis et al. 2002; Malchow 1997). Altogether, such models allow us to estimate not only how resident communities might shift upon the introduction of a new species, but also how fast we expect these changes to take place.

The mathematical foundations for IGP can be found in Holt and Polis (1997), where a three-species IGP network is considered. There, we have two consumers of a single biotic resource, with a predation relation among themselves, as displayed in Fig. 1. Such predation relation allows coexistence between both consumers, in cases which otherwise would be unattainable due to competitive exclusions (Tilman et al. 1990; Klausmeier and Tilman 2002). The precise conditions in which coexistence is possible depend on how large is resource productivity/carrying capacity, and on the intraguild prey (IG prey) being a stronger exploitative competitor than intraguild predator (IG predator) (Holt and Polis 1997. Following Tilman et al. (1990), the latter translates into IG prey leading the resource to lower populational levels than IG predator (when each consumer is set with resource alone). Beyond these results, Holt and Polis (1997) highlight many venues in which the theory can be pushed forward to explain other potential coexistence mechanisms, such as considering age structure, adaptive behaviors, and spatial dynamics, such as dispersal and habitat heterogeneity.

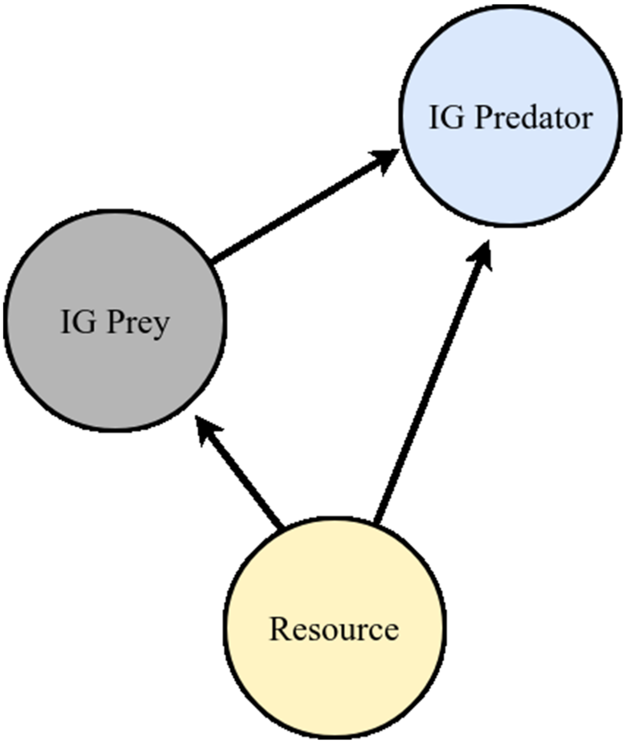

Fig. 1 A three-species intraguild predation network diagram

Notably, reaction diffusion equations have been also developed and applied to study heterogeneous landscapes in Shigesada et al. (1986), with the landscape being composed of two patch types that are arranged periodically over the real line. The work is extended to account for habitat preferences in Maciel and Lutscher (2013), following Ovaskainen and Cornell (2003) to describe individual movement at the interface between different patches, leading to interface conditions that are discontinuous in population density, but continuous in its flux. It is also possible to obtain approximate results for RDE models in periodic landscapes following Yurk and Cobbold (2018) and assuming the dynamics inside a pair of patches occur at a much smaller time scale than that of the whole landscape. With this method, Maciel and Lutscher (2018) investigated how movement behaviors can cause competitive reversals[1] between two competing species, revealing possible regime shift mechanisms based on movement behavior and landscape heterogeneity.

Although some insightful results for IGP in spatial ecology context are present in literature (Bampfylde and Lewis 2007; Amarasekare 2007; Hall 2010), accounting for resource population levels and dispersal simultaneously is

---

[1] When the weaker competitor, by exhibiting a more efficient dispersal behavior than its competitor, can potentially exclude or coexist with it Cantrell et al. (1998).

lacking, with both being potential key processes to understanding coexistence and exclusion regimes. Also, measuring speeds of invasion of a consumer species can unravel how fast possible regime shifts take place, and verifying the formation of spatial profiles, such as traveling wave solutions, can reveal to which novel regimes resident communities will shift to. Understanding the homogeneous landscape problem can also provide expectations for the large spatio-temporal scale for IGP in heterogeneous landscapes, in which patch preference behavior of resource and consumer populations can be accounted for explicitly, and possibly mediate competitive reversals, which in IGP communities would mean shifting coexistence regimes into exclusion ones and vice-versa (Holt and Polis 1997; Polis and Holt 1992).

In this work, we consider a version of the classical IGP model by Holt and Polis (1997) with added ecological diffusion terms to account for movement in homogeneous and heterogeneous landscapes. In Section“Intraguild predation in homogeneous landscapes,” we present the model in homogeneous landscapes and measure invading speeds as well as display some of the regimes found. In Section“Intraguild predation in heterogeneous landscapes,” we present the corresponding model in heterogeneous/periodic landscapes; following Yurk and Cobbold (2018); Cobbold et al. (2022), we perform the homogenization technique, and drawing correspondence with our findings in the homogeneous landscape model, we determine conditions for mutual invasibility in the large spatio-temporal scales. Finally, in Section“Discussion,” we discuss our results and present future venues of research.

Intraguild predation in homogeneous landscapes

Model

We consider that population densities vary in continuous time, t, and space, x, and denote IG prey density as $C_1 \equiv C_1(t,x)$, IG predator as $C_2 \equiv C_2(t,x)$, and the shared resource as $R \equiv R(t,x)$. In our model, every species move with “ecological” diffusion as in Ovaskainen and Cornell (2003); Maciel and Lutscher (2013), predation relations are linear, while consumers are subject to natural mortality and resource grows and reproduces according a density-dependent growth function. The model equations are then

$$\begin{cases} \partial_t C_1 = \partial_x^2(D_1C_1) + b_1C_1R - \alpha C_1C_2 - \delta_1 C_1, \\ \partial_t C_2 = \partial_x^2(D_2C_2) + b_2C_2R + \beta C_1C_2 - \delta_2 C_2, \\ \partial_t R \ = \partial_x^2(D_R R) + G(R) - a_1C_1R - a_2C_2R, \end{cases} \tag{1}$$

defined on $(t,x) \in (0,T) \times \mathbb{R}_+$, where a_i is the attack rate of consumer i upon the resource, and b_i is the conversion rate of resource into new consumers of species i.[2] The natural mortality of consumer i is denoted δ_i, and α is the attack rate of IG predator upon IG prey, while β its conversion rate. The diffusion coefficient of consumer i is D_i, while the diffusion coefficient of resource is D_R.

Finally, in Eq. 1, the function $G(R)$ describes how resource grows. We will assume that $G(R) \geq 0$ for $0 \leq R \leq R^*$ and that $G(R) < 0$ for $R > R^*$, such that $G(R^*) = 0$, i.e., resource population grows in the absence of consumers until it attains density R^*. Also, we assume that $R\partial_R G(R) < G(R)$ for $R > 0$, such that resource alongside a single consumer attain stationary states in the model without spatial structure. Throughout the text, we consider the logistic growth function, i.e, $G(R) = rR(1 - R/K)$, where K is the carrying capacity and r the intrinsic growth rate. However, other choices of growth functions that satisfy the conditions stated have similar qualitative results as we will display here, e.g., the chemostat growth function, i.e., $G(R) = \nu - rR$, where ν is the productivity of the system and r resource removing rate, which is often used to model abiotic resources (Klausmeier and Tilman 2002).

Using the change of variables $\tau = rt$, $y = \sqrt{r/D_R}x$, $u_1 = (\beta/r)C_1$, $u_2 = (\alpha/r)C_2$, and $u_\rho = R/\sqrt{R_1^*R_2^*}$, where $R_i^* = \delta_i/b_i$ is the resource level under exclusive presence of consumer i, we set our equations to

$$\begin{cases} \partial_\tau u_1 = d_1\partial_y^2 u_1 + \gamma m_1 u_1\left(u_\rho - \dfrac{1}{\gamma}\right) - u_1u_2, \\ \partial_\tau u_2 = d_2\partial_y^2 u_2 + \dfrac{m_2u_2}{\gamma}(u_\rho - \gamma) + u_1u_2, \\ \partial_\tau u_\rho = \partial_y^2 u_\rho + f(u_\rho) - e_1u_1u_\rho - e_2u_2u_\rho, \end{cases} \tag{2}$$

where the new quantities are $\gamma = \sqrt{R_2^*/R_1^*}$, $e_1 = a_1/\beta$, $e_2 = a_2/\alpha$, $f(u_\rho) = G(\sqrt{R_1^*R_2^*}u_\rho)/(r\sqrt{R_1^*R_2^*})$, leading to a rescaled carrying capacity $K \leftarrow K/\sqrt{R_1^*R_2^*}$, $d_i = D_i/D_R$ and $m_i = \delta_i/r$. Coexistence regimes are only possible if $\gamma > 1$, which is a competition outcome measure, i.e., whenever $\gamma > 1$ ($\gamma < 1$), IG prey (IG predator) is the stronger competitor.

Invasion regimes and community formation

Now, we consider consumer-resource and IGP communities formed upon introduction of either IG prey or IG predator into a landscape where either resource is established alone or alongside a resident consumer. We consider a small invading population, initially confined in limited space. Then, we linearize the equations around the invader-free fixed points

---

[2] In fact, b_i/a_i is the actual conversion rate, but we address b_i as it for short.

in the sense of the spatially unstructured model. These equations then represent a low density of the invading population at the leading edge and allow us to estimate the minimal spreading speeds, which in turn give us invasibility criteria.

Importantly, successful invasion leads to shifts in the community. In the case of shifts between IG prey and IG predator, such that the former is excluded, the single consumer and resource fixed point is never a center because of our choice of resource growth function (no sustained oscillations are possible); however, the coexistence fixed point can be either stable or a center of oscillations (see Holt and Polis 1997 for a detailed description of fixed points).

Consumer invades resource inhabited landscape

To start, we consider a landscape where resource is established at $u_\rho^* = \bar{u}_\rho,\ f(\bar{u}_\rho) = 0$, and a small density of IG prey initially localized in finite space is invading. IG prey population at the leading edge, where $u_1 \approx 0$, is described by the linearized equation

$$\partial_\tau u_1 = d_1 \partial_y^2 u_1 + u_1 m_1 \gamma \left(\bar{u}_\rho - \frac{1}{\gamma} \right), \tag{3}$$

which yields the minimal spreading speed

$$\hat{c}_{1\to\rho} = 2\sqrt{d_1 m_1 \gamma \left(\bar{u}_\rho - \frac{1}{\gamma} \right)}. \tag{4}$$

Similarly, IG predator (u_2) invading a resource inhabited landscape will have minimal spreading speed

$$\hat{c}_{2\to\rho} = 2\sqrt{\frac{d_2 m_2}{\gamma} (\bar{u}_\rho - \gamma)}. \tag{5}$$

Since a single consumer invading a resource inhabited landscape has linearly determined speed (Lewis et al. 2016; Owen and Lewis 2001), we have that the asymptotic speeds of invasions equal the minimal ones, i.e., $c^*_{i\to\rho} = \hat{c}_{i\to\rho}$. Note that spreading speeds are only real valued for $\bar{u}_\rho > \gamma^{-1}$ in the case of IG prey and $\bar{u}_\rho > \gamma$ in the case of IG predator. These set thresholds on parameters of $f(u_\rho)$. For the logistic growth function, we have $\bar{u}_\rho = K$. Then, for $K > K_{1\to\rho} = \gamma^{-1}$ ($K > K_{2\to\rho} = \gamma$), the landscape can be invaded by IG prey (IG predator).

An example of successful invasion is illustrated in Fig. 2b for IG prey (IG predator). Note that as IG prey (resp. IG predator) spreads, the resource level shifts from the carrying capacity K to γ^{-1} (resp. γ). Also, the solutions present the same spatial pattern at different times, i.e., they are traveling wave solutions of the consumer-resource problem, connecting the resource only fixed point at $y \to \infty$ to the resource-consumer fixed point at $y \to 0$.

IG predator invades IG prey and resource inhabited landscape

When resource is established alongside one of the consumers, however, invasibility criteria change. We start with the case of resource and IG prey stable at levels $u_\rho^* = 1/\gamma$ and $u_1^* = \gamma f(\gamma^{-1})/e_1$ and consider a small density of IG predator

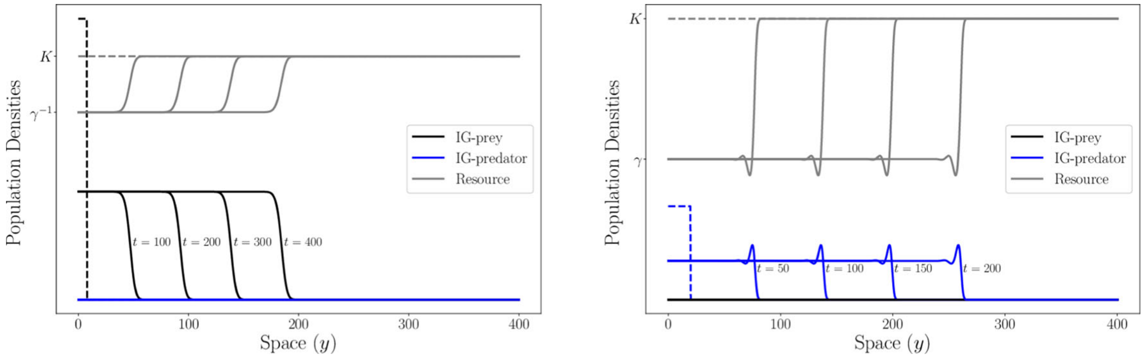

(a) IG prey invades a resource inhabited landscape.

(b) IG predator invades a resource inhabited landscape.

Fig. 2 Single consumer invading a resource only inhabited landscape, represented as solutions at different times t. Gray lines are resource, while black (blue) lines are IG prey (IG predator); color matching dashed lines are initial conditions. Parameters are $2D_1 = 2D_2 = D_R = 0.6$ (space is not rescaled in the figure), $m_1 = 2m_2 = 2e_1 = e_2 = 1.2$ and $\gamma = 1.5$. In **a**, $K = 0.87$, while in **b**, $K = 3$. We use Neumann boundary conditions on both spatial domain extremities invaders localized in a finite space. The linearized equation at the leading edge, where $u_2 \approx 0$, is

$$\partial_\tau u_2 = d_2 \partial_y^2 u_2 + u_2 \left(\frac{m_2}{\gamma} \left(\frac{1}{\gamma} - \gamma \right) + \frac{\gamma}{e_1} f(\gamma^{-1}) \right), \quad (6)$$

yielding minimal speed

$$\hat{c}_{2\to(1,\rho)} = 2\sqrt{\frac{D_2 \gamma}{e_1} \left(f(\gamma^{-1}) - \frac{m_2 e_1}{\gamma^2} \left(\gamma - \frac{1}{\gamma} \right) \right)}. \quad (7)$$

Under the assumption that the minimal spreading speed is the asymptotic one, IG predator invades a landscape inhabited by resource and IG prey given

$$f(\gamma^{-1}) > f_{2\to(1,\rho)} = \frac{m_2 e_1}{\gamma^2} \left(\gamma - \frac{1}{\gamma} \right), \quad (8)$$

which in turn sets new thresholds for parameter values of f. For logistic growth, the carrying capacity must follow:

$$K > K_{2\to(1,\rho)} = \frac{1}{\gamma(1 - \gamma f_{2\to(1,\rho)})}. \quad (9)$$

In the case $\gamma < 1$, condition Eq. 8 is always satisfied, so that IG predator always invades and competitively excludes IG prey. For $\gamma > 1$, in the parameter region $K_{1\to\rho} < K < K_{2\to(1,\rho)}$, we have that only IG prey is able to invade the landscape, while in $K > K_{2\to(1,\rho)}$, IG predator is able to invade the landscape, and, depending on the precise value of K, IG prey either coexists alongside IG predator (see Fig. 3a) or is excluded (Fig. 3b). Note that, for $\gamma > 1$, we have $K_{2\to(1,\rho)} < K_{2\to\rho}$, so the presence of a resident IG prey population facilitates IG predator invasion for these carrying capacity values.

In Fig. 3a and b, we see spatial patterns being formed from $t = 50$ to $t = 100$ and maintained at longer times. In Fig. 3a, the traveling wave solution connects the IG prey and resource fixed point at $y \to \infty$ to the coexistence one in $y \to 0$, while in Fig. 3b, it connects the IG prey and resource fixed point to the IG predator and resource fixed point.

IG prey invades IG predator and resource inhabited landscape

Finally, we consider a landscape inhabited by resource and IG predator, at stable densities $u_\rho^* = \gamma$ and $u_2^* = \gamma^{-1} f(\gamma)/e_2$. A small density of IG prey, $u_1 \approx 0$, is described by the linearized equation

$$\partial_\tau u_1 = d_1 \partial_y^2 u_1 + u_1 \left(m_1 \gamma \left(\gamma - \frac{1}{\gamma} \right) - \frac{1}{\gamma e_2} f(\gamma) \right), \quad (10)$$

and has minimal speed

$$\hat{c}_{1\to(2,\rho)} = 2\sqrt{\frac{D_1}{\gamma e_2} \left(m_1 e_2 \gamma^2 \left(\gamma - \frac{1}{\gamma} \right) - f(\gamma) \right)}, \quad (11)$$

yielding yet another threshold for f in which IG prey is able to invade the landscape, given by

$$f(\gamma) < f_{1\to(2,\rho)} = m_1 e_2 \gamma^2 \left(\gamma - \frac{1}{\gamma} \right). \quad (12)$$

The threshold for carrying capacity is

$$K < K_{1\to(2,\rho)} = \frac{\gamma}{1 - \gamma^{-1} f_{1\to(2,\rho)}}. \quad (13)$$

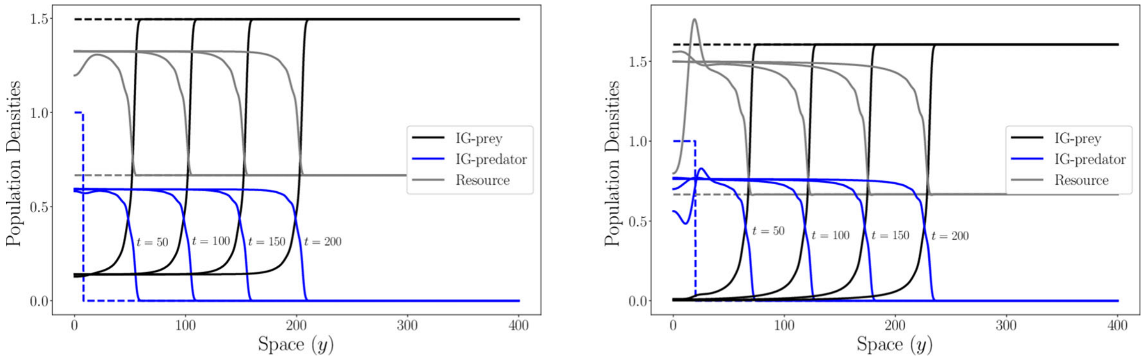

(a) Coexistence after IG predator invasion

(b) Exclusion of IG prey after IG predator invasion.

Fig. 3 IG predator invading a IG prey and resource inhabited landscape, represented as solutions at different times t. Gray lines are resource, while black (blue) lines are IG prey (IG predator); color matching dashed lines are initial conditions. Parameters are $2D_1 = 2D_2 = D_R = 0.6$, $m_1 = 2m_2 = 2e_1 = e_2 = 1.2$, and $\gamma = 1.5$. In **a**, $K = 6.5$, while in **b**, $K = 18$. We use Neumann boundary conditions on both spatial domain extremities and present only the right moving part of the solution

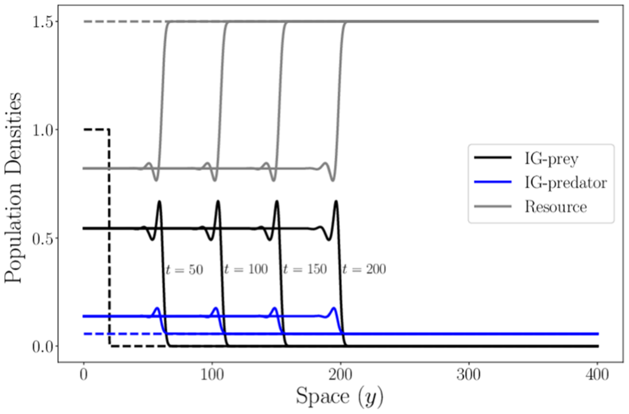

Fig. 4 IG prey invading a IG predator and resource inhabited landscape, represented as solutions at different times t. Gray lines are resource, while black (blue) lines are IG prey (IG predator); color matching dashed lines are initial conditions. Parameters are $2D_1 = 2D_2 = D_R = 0.6$, $m_1 = 2m_2 = 2e_1 = e_2 = 1.2$, and $\gamma = 1.5$, $K = 1.6$. Traveling wave solutions connect the resident IG predator and resource fixed point to the coexistence one. We use Neumann boundary conditions on both spatial domain extremities and present only the right moving part of the solution

For $\gamma < 1$, i.e., when IG prey is not the best competitor, its minimal spreading speed is never real valued. Assuming that the minimal spreading speed is the asymptotic one, we have that IG prey is never able to invade. For $\gamma > 1$, $K_{2\to(1,\rho)} < K < K_{1\to(2,\rho)}$ is a mutual invasibility region, i.e., IG prey can invade an IG predator occupied landscape and vice-versa, leading to a region of coexistence between both consumers (see Fig. 4). The region $K > K_{1\to(2,\rho)}$ IG prey can no longer invade an IG predator occupied landscape, and, in turn, IG predator invasions lead to IG prey exclusion, as previously shown in Fig. 3. Also for $\gamma > 1$, we have $K_{2\to(1,\rho)} < K_{2\to\rho}$, and IG prey can never competitively exclude a resident IG predator population upon invasion.

When the coexistence fixed point is unstable and has maintained oscillations, the system can display dynamical stabilization (Malchow and Petrovskii 2002; Petrovskii and Malchow 2000). In Fig. 5, as the front of invasion advances with speed $c_{i\to(j,\rho)}$, the interface between the dynamical stability region and oscillatory regime also advances in space, but with a smaller speed than the front, such that the length of the dynamical stability region is increasing throughout invasion, similar to what is found in Malchow and Petrovskii (2002).

Asymptotic spreading speeds

We assumed that the minimal spreading speeds correspond to the asymptotic ones. Measuring the spreading speeds numerically (dots in Fig. 6a–d) reveals that, for the explored region of parameter space, this is indeed the case, i.e., the asymptotic spreading speeds equal the minimal ones (solid lines in figures 6a–d).

Note that increasing carrying capacity (Fig. 6a) increases IG predator spreading speed while decreases IG prey spreading speed, as expected, since we have a lower threshold for IG predator invasion in terms of carrying capacity ($K_{2\to(1,\rho)}$) and an upper threshold for IG prey invasion ($K_{1\to(2,\rho)}$). Increasing the invading species diffusivity (Fig. 6b) increases both consumers spreading speeds, as expected.

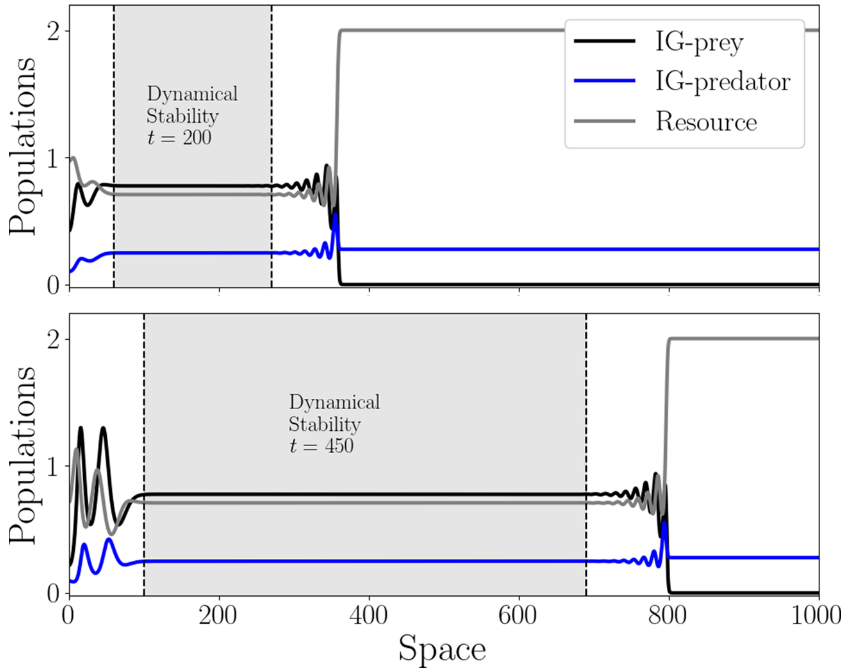

Fig. 5 IG prey invasion leading to dynamical stability (light gray colored region) at $t = 200$ (top) and $t = 450$ (bottom). Parameters used are $K = 3$, $\gamma = 2$, and $e_2 = 2e_1 = m_1 = 2m_2 = 1.2$, $D_1 = D_2 = D_R = 0.5$

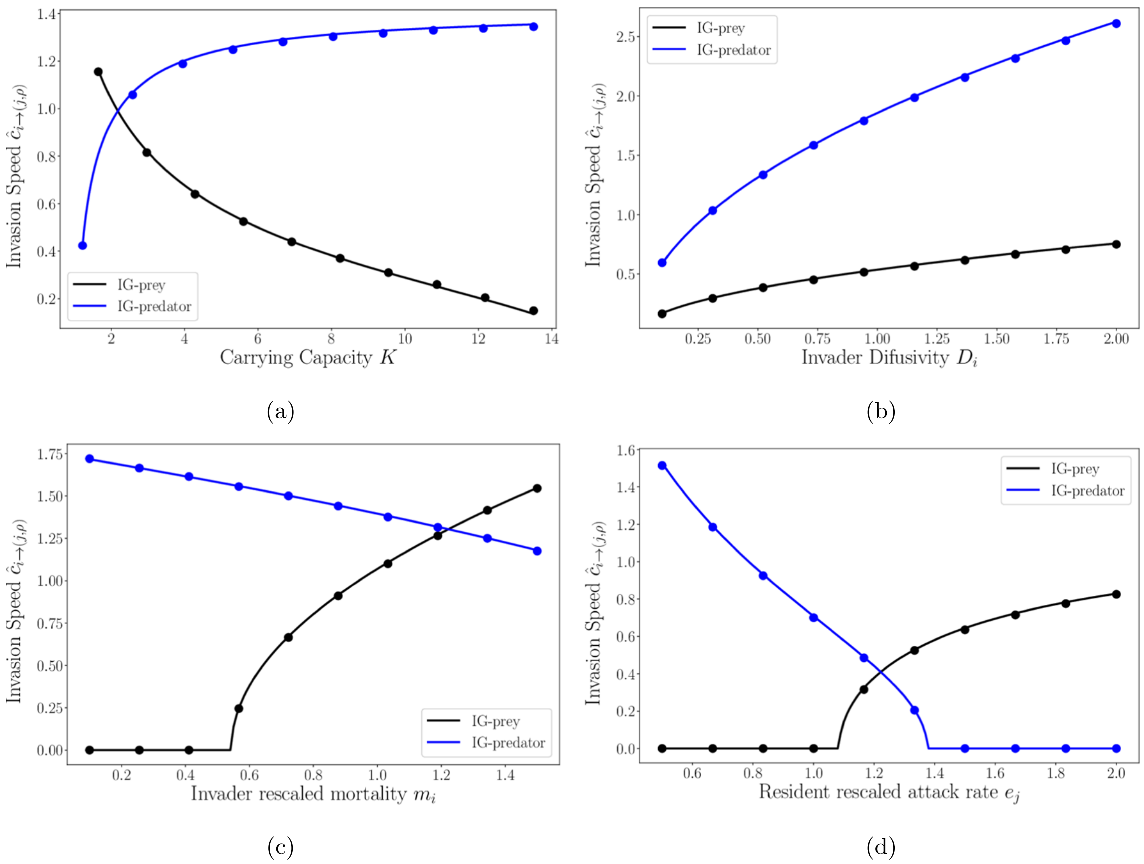

Fig. 6 Numerical (dots) and linearly obtained (lines) spreading speeds for IG prey (black, Eq. 11) and IG predator (blue, Eq. 7). We always analyze the cases of invasion upon a consumer-resource community. We have speed as a function of carrying capacity in **a**, diffusivity in **b**, mortality in **c**, and attack rate in **d**. Parameters used, with the exception of the varying ones on the x axis in each of their respective figures, are $D_1 = D_2 = D_R = 0.5$, $\gamma = 1.5$, $m_2 = 2m_1 = 2e_1 = e_2 = 1.2$, $K = 3$

Spreading speeds behavior in respect to m_i and e_i is not trivial. Note that increasing rescaled mortalities m_i and resident consumer attack rates upon resource e_j produce opposite behaviors on IG prey and IG predator. The main reason lies in the fact that, at the leading edge, the net effect of competition for resource is positive (negative) in IG prey (IG predator). Since the net effect of competition in consumer i is proportional to m_i, increases in m_1 increase IG prey spreading speed, while the opposite holds for IG predator. A similar discussion can be made in terms of e_i and the net effect of intraguild predation at the leading edge. While increasing e_1 decreases the total available IG prey for the consumption of an invading IG predator, thus, reducing its spreading speed, increasing e_2 decreases the total amount of IG predator, reducing predation pressure on an invading IG prey and allowing it to spread with faster speeds.

To illustrate the effects of invasion leading to both regimes on the spreading speeds, we calculate numerical spreading speeds (dots in Fig. 7) and compare them to the ones obtained from linearization (solid lines in Fig. 7) in a parameter region where the coexistence fixed point is unstable (region $\gamma > 2$ in Fig. 7). We observe that, although traveling wave solu-

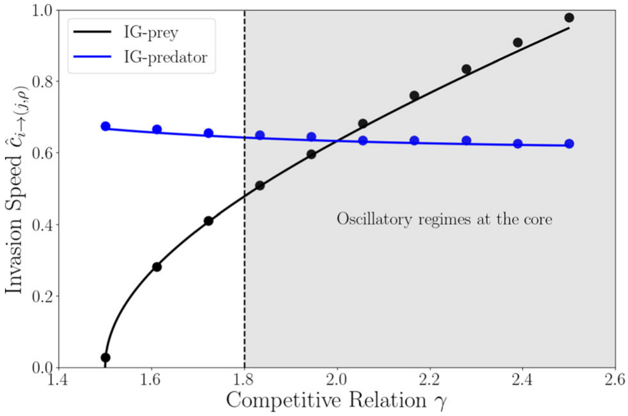

Fig. 7 Asymptotic spreading speeds for different values of γ. In the region $\gamma > 1.8$ (roughly), dynamic stabilization regimes are possible. The numerically obtained speeds (dots) match expressions Eqs. 7 and 11 (lines). Parameters used are $K = 5$ and $e_2 = 2e_1 = m_1 = 2m_2 = 1.2$, $D_1 = D_2 = D_R = 0.5$

tions are not being formed, the spreading speeds are still linearly determined and expressions Eqs. 7 and 11 provide accurate estimates. This was expected, since it also holds in the case of dynamical stabilization regimes of predator–prey models (Malchow and Petrovskii 2002).

Intraguild predation in heterogeneous landscapes

Model

We follow Maciel and Lutscher (2013); Yurk and Cobbold (2018); Cobbold et al. (2022) closely. We let the space be composed of two types of patches, 1 and 2, of sizes l_1 and l_2, respectively, displaced periodically on the real line. We denote the densities of IG prey inside patches of the j-th type as C_{1j}, while for IG predators and resource, we use C_{2j} and R_j, respectively. The dynamics of these populations on a patch of type j are given by

$$\begin{cases} \partial_t C_{1j} = \partial_z^2(D_{1j}C_{1j}) + \mathcal{F}_{1j}, \\ \partial_t C_{2j} = \partial_z^2(D_{2j}C_{2j}) + \mathcal{F}_{2j}, \; z \in T_j \\ \partial_t R_j = \partial_z^2(D_{Rj}R_j) + \mathcal{F}_{Rj}, \end{cases} \tag{14}$$

where T_j is the set of points within patches of type j, i.e.,

$$T_1 = \{z \in \mathbb{R} \mid m(l_1+l_2) < z < m(l_1+l_2)+l_1 \; \forall \, m \in \mathbb{Z}\}, \tag{15}$$

$$T_2 = \{z \in \mathbb{R} \mid m(l_1+l_2) - l_2 < z < m(l_1+l_2) \; \forall \, m \in \mathbb{Z}\}, \tag{16}$$

and $\mathcal{F}_{ij} \equiv \mathcal{F}_{ij}(C_{1j}, C_{2j}, R_j)$, $i = 1, 2, R$, are the growth functions of species i in a patch of type j. Following our model in homogeneous space Eq. 1 and letting intraguild predation relations occur in both patches, we have

$$\mathcal{F}_{1j}(C_{1j}, C_{2j}, R_j) = b_{1j}C_{1j}R_j - \alpha_j C_{1j}C_{2j} - \delta_{1j}C_{1j} \tag{17}$$

$$\mathcal{F}_{2j}(C_{1j}, C_{2j}, R_j) = b_{2j}C_{2j}R_j + \beta_j C_{1j}C_{2j} - \delta_{2j}C_{2j} \tag{18}$$

$$\mathcal{F}_{Rj}(C_{1j}, C_{2j}, R_j) = G_j(R_j) - a_{1j}C_{1j}R_j - a_{2j}C_{2j}R_j, \tag{19}$$

with symbols maintaining their definition as in Eq. 1, but now containing an extra index, j, to denote the patch type in which they are valid. The same is true for the diffusion coefficients D_{ij}. Also, we keep G_j, $j = 1, 2$, as a logistic growth function,[3] with intrinsic growth rate r_j and carrying capacity K_j. For the description of parameters and their correspondence to the homogeneous model Eq. 1, check Table 1.

At the interface z_m of patches of type 1 and 2, we assume continuous flux, but discontinuous densities, to account for habitat preference (Ovaskainen and Cornell 2003; Maciel and Lutscher 2013), leading to

$$\begin{cases} C_{11}(z_m^+, t) \;\; = \;\; k_1 C_{12}(z_m^-, t) \\ D_{11}\partial_z C_{11}(z_m^+, t) = D_{12}\partial_z C_{12}(z_m^-, t) \end{cases} \tag{20}$$

where $z_n = n(l_1 + l_2) + \zeta_n l_1$, $\zeta_n = 1$ ($\zeta_n = 0$) if n is odd (even), and k_1 is the IG prey density effective patch preference. We proceed similarly for IG predator and resource populations to write their interface conditions and define their patch preferences, k_2 and k_R, respectively.

We follow Maciel and Lutscher (2013) to set

$$k_i = \frac{D_{i2}}{D_{i1}} \frac{\alpha_i}{1 - \alpha_i}, \tag{21}$$

where $\alpha_i \in (0, 1)$ is the probability of species i, $i = 1, 2, R$, to move from the interface into a type 1 patch.

It is helpful to write the model Eq. 14 in a shorter notation. We define the piece-wise constant (in z) functions $D_i(z) = D_{ij}$, $z \in T_j$ and $\mathcal{F}_i(z, \cdot) = \mathcal{F}_{ij}(\cdot)$, $z \in T_j$, to write

$$\begin{cases} \partial_t C_1 = \partial_z^2(D_1(z)C_1) + \mathcal{F}_1(z, \cdot), \\ \partial_t C_2 = \partial_z^2(D_2(z)C_2) + \mathcal{F}_2(z, \cdot), \\ \partial_t R = \partial_z^2(D_R(z)R) + \mathcal{F}_R(z, \cdot). \end{cases} \tag{22}$$

Of course, Eq. 22 is only equivalent to Eq. 14 when interface conditions Eq. 20 are accounted for. However, this notation allows us to quickly address population densities C_1, C_2, and R in the landscape level (across multiple different patches).

Homogenization technique

We proceed with a multiscale analysis and approximation method following Yurk and Cobbold (2018); we will briefly outline the method, but refer to the original study for more details. Also, we will describe the methods in terms of a single species, C_1, but the proceedings are the same for C_2 and R and are to be taken simultaneously.

We define the large scale x and the small scale $z = x/\ell$, with $\ell = l_1 + l_2 \ll 1$ in the large scale, and assume that population densities depend on both x and z, leading to $C_1 \equiv C_1(x, z, t)$, the IG prey density in both. Expanding such solutions in ℓ, we get

$$C_1(x, z, t) = \sum_{q=0}^{\infty} \ell^q C_1^{(q)}(x, z, t), \tag{23}$$

and assuming x and z are independent, we have $\partial_z \to \partial_x + \frac{1}{\ell}\partial_z$. When substituting the expanded solution and the change of variables to Eq. 14 with interface conditions Eq. 20, we

---

[3] Here, the choice of logistic growth function reflects a living resource species that actively moves and selects between different patches.

Table 1 Symbol correspondence for parameters on models Eqs. 1, 14, and 25

Parameter/variable	Homogeneous Landscape	Heterogeneous Landscape (small scale)	Heterogeneous Landscape (homogenized)
Population densities	C_1, C_2, R	C_{1j}, C_{2j}, R_j	$\hat{C}_1, \hat{C}_2, \hat{R}$
(Effective) diffusion	D_i	D_{ij}	$\hat{D}_i = \hat{l}_i^2 \langle D_i \rangle^{(H)}$
Resource growth	$G(R) = rR(1 - R/K)$	$G_j(R_j) = r_j R_j (1 - R_j/K_j)$	$\hat{G}(\hat{R}) = \langle r \rangle \hat{R}(1 - \hat{R}/\hat{K})$
Intrinsic growth rate	r	r_j	$\langle r \rangle = \frac{l_1 r_1 + l_2 r_2 / k_R}{\ell_R}$
Carrying capacity	K	K_j	$\hat{K} = \frac{\langle r \rangle \ell_R^2}{l_1 r_1 / K_1 + l_2 r_2 / (K_2 k_R^2)}$
Death rate	δ_i	δ_{ij}	$\langle \delta_i \rangle = \frac{l_1 \delta_{i1} + l_2 \delta_{i2} / k_i}{\ell_i}$
Attack rate	a_i	a_{ij}	$\langle a_i \rangle = \frac{l_1 a_{i1} + l_2 a_{i2} / (k_R k_i)}{\ell_R}$
Conversion rate	b_i	b_{ij}	$\langle b_i \rangle = \frac{l_1 b_{i1} + l_2 b_{i2} / (k_R k_i)}{\ell_i}$
IGP attack rate	α	α_j	$\langle \alpha \rangle = \frac{l_1 \alpha_1 + l_2 \beta_2 / (k_1 k_2)}{\ell_1}$
IGP conversion rate	β	β_j	$\langle \beta \rangle = \frac{l_1 \beta_1 + l_2 \beta_2 / (k_1 k_2)}{\ell_2}$

find a system of coupled equations that can be solved for $C_1^{(0)}, C_1^{(1)}, C_1^{(2)}$.

The leading order of the expansion, $C_1^{(0)}$, is given by

$$C_1^{(0)}(x, z, t) = \frac{\hat{C}_1(x, t)}{h_1(z)}, \tag{24}$$

where $h_1(z) = 1$ ($h_1(z) = k_1$) for $z \in T_1$ ($z \in T_2$). Applying the same procedure to C_2 and R, we arrive in a similar expression for $C_2^{(0)}$ and $R^{(0)}$, with $h_2(z)$ and $h_R(z)$ defined in the same fashion as $h_1(z)$. Since $h_i(z) > 0 \, \forall i, \ z$, the population densities are strongly dependent on $\hat{C}_1, \ \hat{C}_2$ and $\hat{R}$, which are obtained by solving

$$\begin{cases} \partial_t \hat{C}_1 = \hat{l}_1^2 \langle D_1 \rangle^{(H)} \partial_x^2 \hat{C}_1 + \langle \mathcal{F}_1 \rangle (\hat{C}_1, \hat{C}_2, \hat{R}), \\ \partial_t \hat{C}_2 = \hat{l}_2^2 \langle D_2 \rangle^{(H)} \partial_x^2 \hat{C}_2 + \langle \mathcal{F}_2 \rangle (\hat{C}_1, \hat{C}_2, \hat{R}), \\ \partial_t \hat{R} \ = \hat{l}_R^2 \langle D_R \rangle^{(H)} \partial_x^2 \hat{R} + \langle \mathcal{F}_R \rangle (\hat{C}_1, \hat{C}_2, \hat{R}), \end{cases} \tag{25}$$

where $\hat{l}_i$, $\langle D_i \rangle^{(H)}$, and $\langle \mathcal{F}_i \rangle$ are the scaled spatial periods, diffusion coefficients, and growth functions of species i in the large scale, respectively. Namely, the scaled periods are given by

$$\hat{l}_i = \frac{\ell}{\ell_i}, \quad \text{with} \quad \ell_i = l_1 + \frac{l_2}{k_i}, \tag{26}$$

while the diffusion coefficients are the harmonic mean between the diffusion coefficients of each habitat, i.e.,

$$\langle D_i \rangle^{(H)} = \frac{\ell_i}{\frac{l_1}{D_{i1}} + \frac{k_i l_2}{D_{i2}}} \tag{27}$$

and the growth functions are the arithmetic mean of $\mathcal{F}_{ij}$, i.e.,

$$\langle \mathcal{F}_i \rangle (\hat{C}_1, \hat{C}_2, \hat{R}) = \frac{1}{\ell_i} (l_1 \mathcal{F}_{i1}(\hat{C}_1, \hat{C}_2, \hat{R}) + l_2 \mathcal{F}_{i2}(\hat{C}_1/k_1, \hat{C}_2/k_2, \hat{R}/k_R)). \tag{28}$$

Rearranging the terms in $\langle \mathcal{F}_j \rangle$, we find that system Eq. 25 can be written in the same form as Eq. 1, i.e.,

$$\begin{cases} \partial_t \hat{C}_1 = \partial_x^2 (\hat{D}_1 \hat{C}_1) + \langle b_1 \rangle \hat{C}_1 \hat{R} - \langle \alpha \rangle \hat{C}_1 \hat{C}_2 - \langle \delta_1 \rangle \hat{C}_1, \\ \partial_t \hat{C}_2 = \partial_x^2 (\hat{D}_2 \hat{C}_2) + \langle b_2 \rangle \hat{C}_2 \hat{R} + \langle \beta \rangle C_1 C_2 - \langle \delta_2 \rangle C_2, \\ \partial_t \hat{R} \ = \partial_x^2 (\hat{D}_R \hat{R}) + \langle G \rangle (\hat{R}) - \langle a_1 \rangle \hat{C}_1 \hat{R} - \langle a_2 \rangle \hat{C}_2 \hat{R}. \end{cases} \tag{29}$$

We organize the definition and correspondence between the heterogeneous landscape homogenized parameters in model Eq. 29 and the homogeneous landscape parameters in model Eq. 1 in Table 1.

With the parameters defined in Table 1, we rescale time, space, and population densities as follows:

$$\begin{gathered} U_1=\tfrac{\langle\beta\rangle}{\langle r\rangle}\hat{C}_1 \qquad U_2=\tfrac{\langle\alpha\rangle}{\langle r\rangle}\hat{C}_2 \qquad U_R=\frac{\hat{R}}{\sqrt{\hat{R}_1^*\hat{R}_2^*}}, \\ t'=\langle r\rangle t \qquad x'=\sqrt{\tfrac{\langle r\rangle}{\hat{D}_R}}\,x \end{gathered} \tag{30}$$

where

$$\hat{R}_i^*=\frac{\langle\delta_i\rangle}{\langle b_i\rangle}=\frac{l_1\delta_{i1}+l_2\delta_{i2}/k_i}{\frac{l_1\delta_{i1}}{R_{i1}^*}+\frac{l_2\delta_{i2}}{R_{i2}^*k_ik_R}}, \tag{31}$$

is the (approximate) resource level when established with only consumer i in an heterogeneous landscape. R_{ij}^* has a similar definition as $\hat{R}_i^*$ (and R_i^* in Eq. 1), but only with respect to the patch type j, i.e., $R_{ij}^*=\delta_{ij}/b_{ij}$, $j=1,2$, and $i=1,2$.

After some algebra, system Eq. 29 can be written as

$$\begin{cases} \partial_{t'}U_1=\sigma_1\partial_{x'}^2U_1+\Gamma M_1U_1\left(U_R-\dfrac{1}{\Gamma}\right)-U_1U_2, \\ \partial_{t'}U_2=\sigma_2\partial_{x'}^2U_2+\dfrac{M_2U_2}{\Gamma}(U_R-\Gamma)+U_1U_2, \\ \partial_{t'}U_R=\partial_{x'}^2U_R+\Phi(U_R)-E_1U_1U_R-E_2U_2U_R, \end{cases} \tag{32}$$

which is precisely in the same form of Eq. 2. The new quantities are

$$\begin{gathered} M_i=\tfrac{\langle\delta_i\rangle}{\langle r\rangle},\ E_1=\tfrac{\langle a_1\rangle}{\langle\beta\rangle},\ E_2=\tfrac{\langle a_2\rangle}{\langle\alpha\rangle}, \\ \sigma_i=\tfrac{\hat{D}_i}{\hat{D}_R},\quad \Gamma=\sqrt{\tfrac{\hat{R}_2^*}{\hat{R}_1^*}},\ \Phi(U_R)=\frac{\hat{G}(\sqrt{\hat{R}_1^*\hat{R}_2^*}U_R)}{\langle r\rangle\sqrt{\hat{R}_1^*\hat{R}_2^*}}, \end{gathered} \tag{33}$$

where we rescale the carrying capacity to $\hat{K}\leftarrow\hat{K}/\sqrt{\hat{R}_1^*\hat{R}_2^*}$.

Mutual invasibility conditions

Since models Eqs. 32 and 2 are in the same form, we expect mutual invasibility of IG prey and IG predator to take place in the same correspondent parameter regions as found for the homogeneous landscapes. This way, we expect mutual invasibility only for $\Gamma>1$, i.e., when the homogenized competitive measure shows that IG prey is the stronger competitor and within a range of effective carrying capacities $\hat{K}$.

The condition $\Gamma>1$, in full form, becomes

$$\gamma_1\gamma_2>\left(\frac{\tilde{\theta}_2k_2k_R+\tilde{\delta}_2l/\tilde{\theta}_2}{k_2+\tilde{\delta}_2l}\right)\left(\frac{\tilde{\theta}_1k_1k_R+\tilde{\delta}_1l/\tilde{\theta}_1}{k_1+\tilde{\delta}_1l}\right)^{-1}, \tag{34}$$

where $l=l_2/l_1$ is the ratio of patch sizes, $\tilde{\delta}_i=\delta_{i2}/\delta_{i1}$ is the ratio of species i death rates in patch 2 and patch 1, $\tilde{\theta}_i=\sqrt{R_{i2}^*/R_{i1}^*}$, the ratio between resource levels in presence of species i in different patch types. Finally, $\gamma_j=\sqrt{R_{2j}^*/R_{1j}^*}$ is the competition outcome measure in patches of type j.

Whenever the right-hand side of inequality Eq. 34 is smaller than unity, mutual invasibility is facilitated and can occur even if $\gamma_j<1$, $j=1,2$, i.e., competitive reversals in favor of IG prey are possible. At the same time, whenever the right-hand side is larger than unity, mutual invasibility is hindered and may not occur even if $\gamma_j>1$, $j=1,2$, i.e., competitive reversals in favor of IG predator are also possible. When the right-hand side is precisely unity, the condition reduces to $\gamma_1>\gamma_2^{-1}$, that is, whenever IG prey is not competitively stronger in one of the patches, it has to overcompensate for it in the other patch.

The possible competitive reversal scenarios found on inequality Eq. 34 depend heavily on all three species patch preferences, k_i, $i=1,2,R$, how patchy the landscape is, given by l, as well as consumer traits ($\tilde{\theta}_i$ and $\tilde{\delta}_i$). To simplify this relation and gain some insight on how habitat preferences govern inequality Eq. 34, we assume $\gamma_1=\gamma_2=\gamma$, which also implies $\tilde{\theta}_1=\tilde{\theta}_2=\tilde{\theta}$, and define $q_R=\tilde{\theta}^2k_R$ and $\eta_i=\tilde{\delta}_i/k_i$. With that, condition Eq. 34 becomes

$$\gamma^2>\left(\frac{q_R+\eta_2l}{1+\eta_2l}\right)\left(\frac{1+\eta_1l}{q_R+\eta_1l}\right)=w(q_R,l,\eta_1,\eta_2). \tag{35}$$

Note that $w(q_R=1,\cdot)=1$, i.e., whenever $q_R=1$, we recover the conditions found in an homogeneous landscape. Moreover,

$$\operatorname{sign}(\partial_{q_R}w)=\operatorname{sign}(\eta_1-\eta_2) \tag{36}$$

such that if $\eta_1>\eta_2$, then w is monotonically increasing in q_R and monotonically decreasing otherwise. Because q_R is monotone in $\tilde{\theta}$ and k_R, w is also monotone in these parameters. Since $w(q_R=1,\cdot)=1$, if w is monotonically increasing in q_R (Fig. 8a), then for $q_R>1$, we have hindered mutual invasibility conditions, $\gamma^2>w(q_R,\cdot)>1$, i.e., γ must be larger than what is expected in an homogeneous landscape. For $q_R<1$, we have facilitated mutual invasibility conditions, $\gamma^2>w(q_R,\cdot)$ with $w(q_R,\cdot)<1$, i.e., γ can be smaller than what is expected in an homogeneous landscape. The opposite holds when w is monotonically decreasing (Fig. 8b).

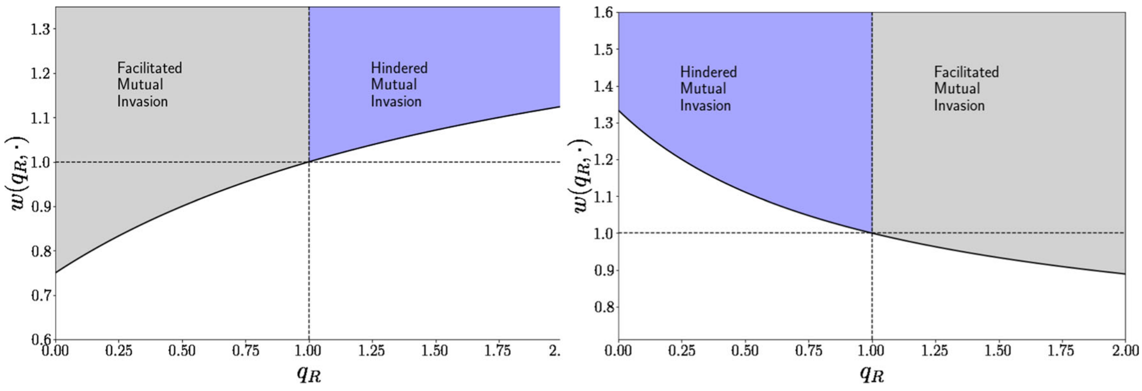

(a) w is monotonically increasing in q_R: $\eta_1 > \eta_2$

(b) w is monotonically decreasing in q_R: $\eta_1 < \eta_2$

Fig. 8 Regimes of facilitated and hindered mutual invasions, depending on how the quantities $\eta_i = \frac{\tilde{\delta}_i}{k_i}$, $i = 1, 2$ relate

The ecological interpretation of inequality Eqs. 35 and 36 is as follows: $\eta_i = \tilde{\delta}_i / k_i$ relates species i patch preference, k_i, and how much larger is its death rate in patches of type 2 compared to type 1, $\tilde{\delta}_i$. Whenever there is a difference between IG prey and IG predator in this relation, then mutual invasibility is hindered or facilitated depending on how unbalanced is resource consumption between different patches, θ, and resource patch preference k_R.

To understand solely the effects of patch preferences, let $\tilde{\delta}_1 = \tilde{\delta}_2, \tilde{\theta} = 1$ and consider the following example: IG prey prefers patches of type 1, and IG predator prefers patches of type 2, such that $k_2 < 1 < k_1$, and therefore, w is monotonically decreasing. The region $k_R > 1$ (resource prefers patches of type 1) leads to a competitive reversal in favor of IG prey whenever $w < \gamma^2 < 1$, while the region $k_R < 1$ (resource prefers patches of type 2) leads to competitive reversals in favor of IG predator whenever $w > \gamma^2 > 1$. The outcomes of the example are reversed when $k_1 < 1 < k_2$, i.e., IG prey and IG predator patch preferences are switched. This way, whichever consumer has their patch preferences aligned with resource species' patch preference can benefit from competitive reversals.

Similarly, we can understand competitive reversal scenarios only considering the death rate ratios, $\tilde{\delta}_i$, and uneven resource consumption between patches, $\tilde{\theta}$, through the following example: Let $k_1 = k_2$ and $k_R = 1$ and consider IG prey have a smaller death rate in patches of type 1 than in patches of type 2, and the opposite for IG predator, such that $\tilde{\delta}_2 < 1 < \tilde{\delta}_1$. With that, w is monotonically increasing in $\tilde{\theta}$. For $\tilde{\theta} < 1$, i.e., resource is less consumed in patches of type 1, we may have competitive reversals in favor of IG prey whenever $w < \gamma^2 < 1$, while $\tilde{\theta} > 1$ favors IG predator if $w > \gamma^2 > 1$. That way, whenever the patch where IG prey dies less is also the one where resource is less consumed, we have facilitated mutual invasibility, while hindered conditions apply when we have the opposite.

We could also discuss similar effects that occur between k_1, k_2 and $\tilde{\theta}$, as well as between $\tilde{\delta}_1, \tilde{\delta}_2$ and k_R, but the outcome would be quite similar. In a general manner, whenever the conditions favor IG prey (IG predator) in some way, the mutual invasibility conditions are facilitated (hindered). To formally write these parameter regions, we define $\delta\eta = \eta_1 - \eta_2$ and write the facilitated, $\mathcal{H}_f$, and hindered, $\mathcal{H}_h$, mutual invasion conditions as quadrants in the parameter space $(q_R, \delta\eta) \in \mathbb{R}_+ \times \mathbb{R}$ defined by

$$\mathcal{H}_f = \{(q_R, \delta\eta) \in \mathbb{R}_+ \times \mathbb{R} | q_R < 1 \text{ and } \delta\eta > 0 \text{ or } q_R > 1 \text{ and } \delta\eta < 0\}, \tag{37}$$

$$\mathcal{H}_h = \{(q_R, \delta\eta) \in \mathbb{R}_+ \times \mathbb{R} | q_R > 1 \text{ and } \delta\eta > 0 \text{ or } q_R < 1 \text{ and } \delta\eta < 0\}. \tag{38}$$

The ratio among patch sizes, l, does not appear in any of the relations discussed so far, but it does play an important role. Again, we focus on the case $\gamma_1 = \gamma_2 = \gamma$, just to simplify expressions and gain some insight.

We have $\Gamma^2 = \gamma^2 / w$, and we note that

$$\lim_{l \to 0} \Gamma(l, \cdot) = \lim_{l \to \infty} \Gamma(l, \cdot) = \gamma, \tag{39}$$

i.e., whenever the landscape is almost homogeneous ($l_1 \gg l_2$ or $l_2 \ll l_1$), we recover the homogeneous mutual invasion conditions.

A quick inspection on the derivative $\partial_l \Gamma^2$ reveals that

$$\text{sign}(\partial_l \{\Gamma^2\}) = \text{sign}\left[(q_R - 1)\delta\eta \left(\frac{\eta_1 \eta_2}{q_R} l^2 - 1 \right) \right], \tag{40}$$

so $\partial_l \Gamma$ switches sign just once, at $l^* = \sqrt{\frac{q_R}{\eta_1 \eta_2}}$, which is therefore the only extreme point of Γ w.r.t l, and limits

Eq. 39 imply Γ is bounded by its extreme, $\Gamma(l = l^*, \cdot)$, and γ. Note that l^* is the maximum point of $\Gamma(l, \cdot)$ whenever $(q_r, \delta\eta) \in \mathcal{H}_f$, and by limits in Eq. 39, we have $\gamma < \Gamma(l, \cdot) \leq \Gamma(l = l^*, \cdot)$. Therefore, if $\gamma > 1$, mutual invasion regimes are possible for any l. In a similar fashion, l^* is a minimum point of $\Gamma(l, \cdot)$ whenever $(q_r, \delta\eta) \in \mathcal{H}_h$, and the limits in Eq. 39 imply $\Gamma(l = l^*, \cdot) \leq \Gamma(l, \cdot) < \gamma$. Therefore, if $\gamma < 1$ mutual invasion regimes are not possible for any l. That is, whenever IG prey (resp. IG predator) is the superior competitor and is benefited by facilitated (resp. hindered) mutual invasion conditions, mutual invasions can (resp. do not) take place regardless of how patchy the landscape is.

Now, assuming that l^* is a maximum point, in order to have $\Gamma(l = l^*, \cdot) > 1$, we must have

$$\gamma^2 > \frac{\frac{\tilde{\delta}_1}{k_1} q_R + \frac{\tilde{\delta}_2}{k_2} - 2\sqrt{q_R \frac{\tilde{\delta}_1}{k_1} \frac{\tilde{\delta}_2}{k_2}}}{\frac{\tilde{\delta}_1}{k_1} + \frac{\tilde{\delta}_2}{k_2} q_R - 2\sqrt{q_R \frac{\tilde{\delta}_1}{k_1} \frac{\tilde{\delta}_2}{k_2}}} = w(q_R, l^*, \eta_1, \eta_2). \tag{41}$$

However, $w(q_R, l^*, \eta_1, \eta_2) < 1$ for $(q_R, \delta\eta) \in \mathcal{H}_f$. By continuity of $\Gamma(l, \cdot)$, whenever

$$w(q_R, l^*, \eta_1, \eta_2) < \gamma^2 < 1, \tag{42}$$

we have competitive reversals in favor of IG prey around a neighborhood of l^* and mutual invasions are possible, i.e., in order to have $\Gamma > 1$ even when $\gamma < 1$, the proportion of patch type lengths must be close to l^*.

The precise extent of l values at which competitive reversals occur is obtained by solving $\Gamma(l = \bar{l}, \cdot) = 1$, which yields $\bar{l}_\pm = \bar{l}_0 \pm \sqrt{\bar{l}_0^2 - l^{*2}}$, where

$$\bar{l}_0 = -\frac{1}{2\eta_1\eta_2}\left(\eta_1 \frac{(\gamma^2 - q_R)}{(\gamma^2 - 1)} + \eta_2 \frac{(\gamma^2 q_R - 1)}{(\gamma^2 - 1)}\right). \tag{43}$$

Note that roots $\bar{l}_\pm$ become negative whenever $\gamma > 1$ and $(q_R, \delta\eta) \in \mathcal{H}_f$. In this regime, mutual invasion becomes possible for any l, as expected.

By assuming that l^* is a minimum, i.e., that hindered mutual invasion conditions take place, we arrive at complementary results. We have

$$w(q_R, l^*, \eta_1, \eta_2) > 1 \text{ for } (q_R, \delta\eta) \in \mathcal{H}_h, \tag{44}$$

and whenever

$$1 < \gamma^2 < w(q_R, l^*, \eta_1, \eta_2), \tag{45}$$

competitive reversals occur in favor of IG predator. Mutual invasions are only possible outside the range $[\bar{l}_-, \bar{l}_+]$, i.e., when the landscape is more homogeneous/less patchy. Also, if $\gamma < 1$ and $(q_R, \delta\eta) \in \mathcal{H}_h$, both $\bar{l}_\pm$ become negative and mutual invasibility is not possible, as expected.

Whenever competitive reversals occur, $(q_R, \delta\eta)$ determines in which direction the reversals are and the roots $l_\pm$ delimit the heterogeneity levels of the landscape necessary for it. Still, mutual invasibility regions only take place within a range of effective carrying capacities, $\hat{K}$. We proceed as in the homogeneous case and define

$$\Phi_{1\to(2,R)} = M_1 E_2 \Gamma^2 \left(\Gamma - \frac{1}{\Gamma}\right), \tag{46}$$

$$\Phi_{2\to(1,R)} = \frac{M_2 E_1}{\Gamma^2}\left(\Gamma - \frac{1}{\Gamma}\right), \tag{47}$$

and with these, the threshold values in $\hat{K}$ become

$$\hat{K}_{1\to R} = \frac{1}{\Gamma}, \tag{48}$$

$$\hat{K}_{1\to(2,R)} = \frac{\Gamma}{1 - \Gamma^{-1}\Phi_{1\to(2,R)}}, \tag{49}$$

$$\hat{K}_{2\to(1,R)} = \frac{1}{\Gamma(1 - \Gamma\Phi_{2\to(1,R)})}, \tag{50}$$

$$\hat{K}_{2\to R} = \Gamma. \tag{51}$$

The mutual invasibility region is delimited by $\hat{K}_{2\to(1,R)} < \hat{K} < \hat{K}_{1\to(2,R)}$, which only exists if $\Gamma > 1$. We investigate these regions in the plane $(\hat{K}, l)$ by plotting the different threshold values $\hat{K}$.. To illustrate the precise effects of competitive reversals, we focus again on $\gamma_1 = \gamma_2 = \gamma$.

First, let us consider the case of competitive reversals in favor of IG prey; we consider $w(q_R, l*, \eta_1, \eta_2) < \gamma < 1$ and $(q_R, \delta\eta) \in \mathcal{H}_f$, to plot Fig. 9. At the limits $\log(l) \to \pm\infty$, the landscape is more homogeneous and heavily composed of a single patch type, and regime shifts from increasing levels of carrying capacity occur only from resource alone (pastel colored) to IG predator and resource communities (blue colored). Note that the $l \in [\bar{l}_-, \bar{l}_+]$ region, when the landscape becomes more patchy, we have $\Gamma > 1$ in the upper plot, corresponding to the l region where IG prey can establish alone with resource (gray colored) and mutual invasions can occur (cyan colored) in the lower plot. All curves are increasing in $\log(l)$ because $k_R < 1/2$, so resource strongly prefers patches of type 1, which length's proportion decreases with increasing l.

To compare the approximation in Fig. 9 with numerical results, we plot the maximum population densities in Fig. 10. For that, we let 10 pairs of patches 1 and 2 of equal size ($l_1 = l_2 = 1$) in order to investigate whether mutual invasibility regimes were indeed observed and vary the carrying capacities in each patch equally. The thresholds found via homogenization technique are quite close to the ones

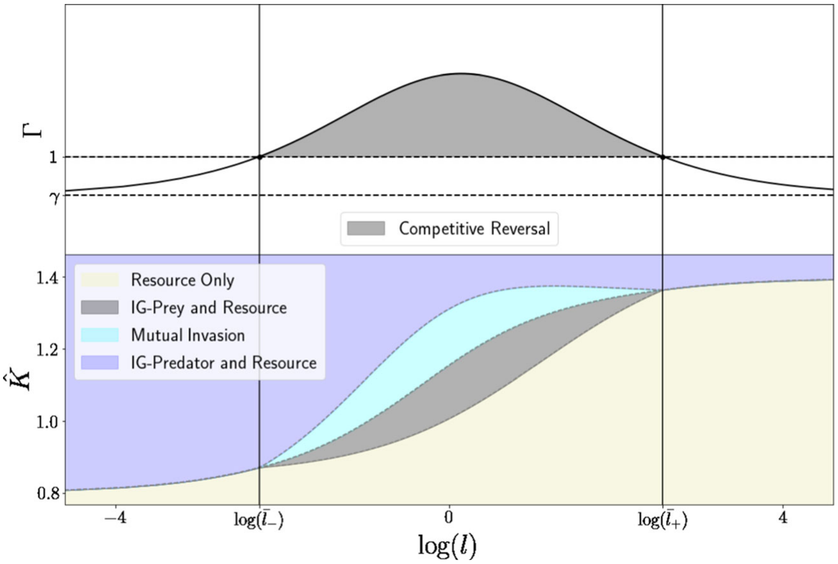

Fig. 9 *Top*: Γ as a function of $\log(l)$. The gray colored region indicates a competitive reversals in favor of IG prey. *Bottom*: Invasibility regimes for different values of $\hat{K}$. The blue region is bounded below by $\hat{K}_{1\to(2R)}$ for $l \in [\bar{l}_-, \bar{l}_+]$ and by $\hat{K}_{2\to R}$ for other values of l; cyan region is comprised by $[\bar{l}_-, \bar{l}_+] \times [\hat{K}_{2\to(1R)}, \hat{K}_{1\to(2R)}]$; gray region is comprised by $[\bar{l}_-, \bar{l}_+] \times [\hat{K}_{1\to(R)}, \hat{K}_{2\to(1R)}]$; the pastel region is the complementary in the $(\hat{K}, \log(l))$ parameter space. *Parameters used*: $\alpha_1 = \alpha_2 = 0.25$, $\beta_1 = \beta_2 = 0.45$, $b_{11} = b_{12} = 0.8$, $b_{21} = 0.85 b_{22} = 0.6$, $\delta_{11} = \delta_{12} = 0.7$ $\delta_{21} = 0.85\delta_{22} = 0.5$, $r_1 = r_2 = 1, 2D_1 = D_2 = 2D_R = 1.4, \alpha_1 = \alpha_R = 1 - \alpha_2 = 0.45$

observed numerically, and mutual invasibility showed to lead to coexistence between IG prey and IG predator.

Now, in the case $1 < \gamma < w(q_R, l*, \eta_1, \eta_2) >$ and $(q_r, \delta\eta) \in \mathcal{H}_h$, we have Fig. 11. The regions of mutual invasibility (cyan colored) and IG prey dominance (gray colored) only exist outside the range $[\bar{l}_-, \bar{l}]$, where $\Gamma > 1$ in the top plot. Inside the interval $[\bar{l}_-, \bar{l}]$, only IG predator is able to invade granted resource carrying capacity is high enough (blue colored), where $\Gamma < 1$, while for low values of carrying capacity, only resource is established in the landscape (pastel colored). This depicts a competitive reversal in favor of IG predator.

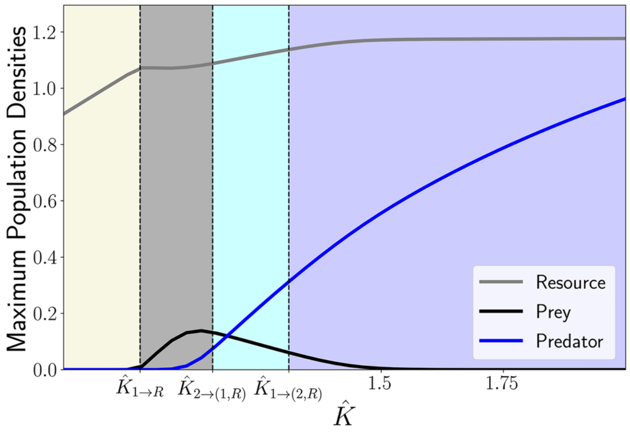

Fig. 10 Numerically obtained maximum population densities for $l = 1$. The colored regions and parameters used are the same as in Fig. 9

Again, we compare the approximation in Fig. 11 with numerical results in Fig. 12. For that, we let 10 pairs of patches 1 and 2 of equal size ($l_1 = l_2 = 1$) in order to investigate whether exclusion regimes were indeed observed and vary the carrying capacities in each patch equally, as before. The IG predator threshold found via homogenization technique is quite close to the one observed numerically.

Discussion

In this work, we analyzed intraguild predation communities in homogeneous and heterogeneous landscapes, studying consumer species invasion dynamics. In an homogeneous landscape, we recover invasibility conditions as expected in Holt and Polis (1997), while also numerically verified that speeds of invasion are linearly determinate. In heterogeneous environments, using an approximation technique, we found competitive reversals between IG prey and IG predators modulated by multiple factors.

In a homogeneous landscape, we have four possible invasion regimes for when the IG prey is the best exploitative competitor. First, neither of the consumers are able to invade, given a really low carrying capacity, then, for higher carrying capacities, we have three distinct ranges: IG prey is able to invade, mutual invasibility between IG prey and IG predator, and IG predator invasions leading to IG prey exclusion and preventing IG prey invasion. For the case where

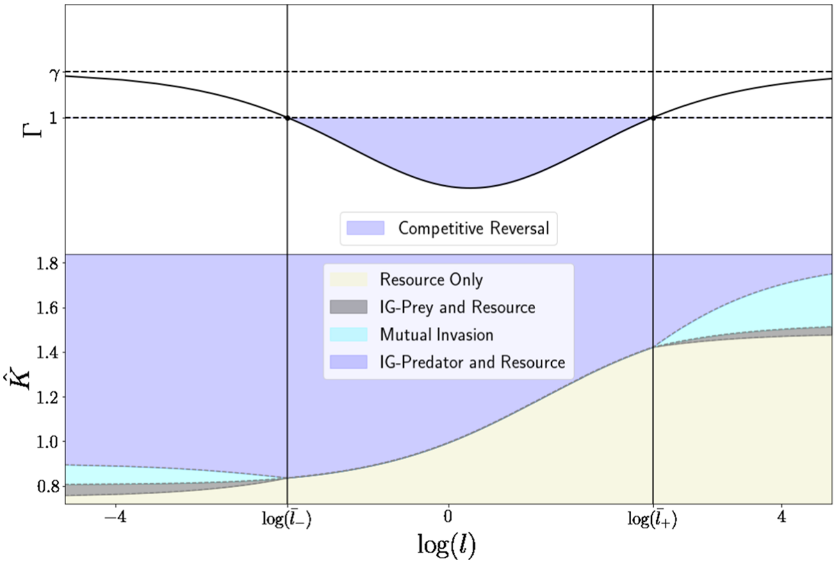

Fig. 11 *Top*: Γ as a function of $\log(l)$. The gray colored region indicates a competitive reversals in favor of IG prey. *Bottom*: Invasibility regimes for different values of $\hat{K}$. The blue region is bounded below by $\hat{K}_{1\to(2R)}$ for $l \in [\bar{l}_-, \bar{l}_+]$ and by $\hat{K}_{2\to R}$ for other values of l; cyan region is comprised by $[\bar{l}_-, \bar{l}_+] \times [\hat{K}_{2\to(1R)}, \hat{K}_{1\to(2R)}]$; gray region is comprised by $[\bar{l}_-, \bar{l}_+] \times [\hat{K}_{1\to(R)}, \hat{K}_{2\to(1R)}]$; the pastel region is the complementary in the $(\hat{K}, \log(l))$ parameter space. *Parameters used*: $\gamma = 1.05$, $\alpha_1 = \alpha_2 = 0.25$, $\beta_1 = \beta_2 = 0.45$, $b_{11} = b_{12} = 0.8$, $b_{21} = 0.85 b_{22} = 0.6$, $\delta_{11} = \delta_{12} = 0.7$ $\delta_{21} = 0.85 \delta_{22} = 0.5$, $r_1 = r_2 = 1$, $2D_1 = D_2 = 2D_R = 1.4$, $\alpha_1 = \alpha_R = 1 - \alpha_2 = 0.45$

IG predator is the best consumer, we only find two regimes, either no consumer invades for really low carrying capacities or IG predator invades for large enough carrying capacities, excluding IG prey whenever it is also present in the landscape, or also preventing IG prey invasion. This is the classical result of Holt and Polis (1997), now revisited in the form of invisibility analysis of spatially structured populations.

Our numerical analysis of the homogeneous landscape model suggests that the different speeds of invasion are linearly determined for a large range of parameter values. This was somehow expected, because invasions in consumer-resource models show linearly determinate speed as well (Petrovskii and Malchow 2000, 1999; Lewis et al. 2016). We show that whenever a successful invasion leads to a shift from the resident community fixed point to a different stable fixed point (in the not spatially structured model sense), we usually have traveling wave solutions connecting these fixed points. We also show that dynamical stability regions can be formed when the coexistence fixed point is unstable, but leave the precise conditions in which such dynamical stability occurs for future research, possibly using the same analysis as in Malchow and Petrovskii (2002), which gets slightly more complicated in a three-species system.

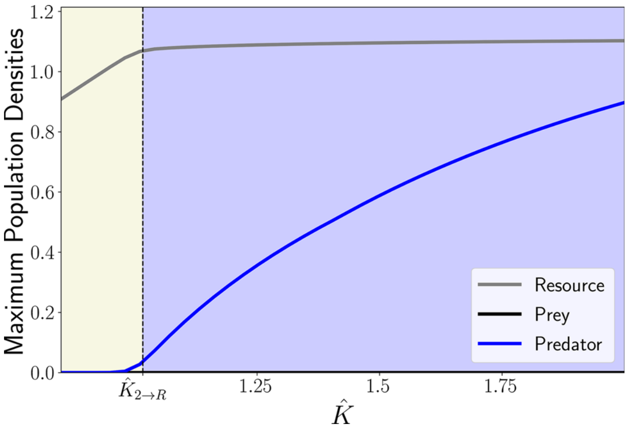

Fig. 12 Numerically obtained maximum population densities for $l = 1$. The colored regions and parameters used are the same as in Fig. 11

We have chosen linear functional responses for predator–prey dynamics, for both consumer-consumer or consumer-resource predation. However, if consumer-resource relations are type II Holling functions (Holling 1959), the single consumer and resource equilibria can be unstable and present oscillations, allowing for coexistence among two consumers without intraguild predation relations (Klausmeier and Tilman 2002; Armstrong and McGehee 1980). The invasibility analysis in this scenario, however, gets much more complicated, and studying invasibility criteria, spreading speeds, and regime shifts both with and without IGP relations is a possible venue for future research.

The same invasibility regions found in homogeneous landscapes are found in periodic landscapes as well. However, they depend on multiple factors, and competitive reversals might occur. Competitive reversals have also been observed in models for interference competition in periodic landscapes in Maciel et al. (2018) and depend exclusively on patchiness, l, and competitor species movement behaviors. Here, we show that, in exploitative competition, resource patch preference is a key factor in order for competitive reversals to occur, either favoring IG prey or IG predator, whichever has its patch preference more aligned with resources or has a lower mortality rate in resource species favored patch, thereby facilitating or hindering mutual invasibility regimes. Competitive reversals can also occur if resource is unevenly consumed between patches. When resource is much less consumed where one of the consumers has a lower mortality rate, that consumer is benefited and can possibly overcome the fact of being the worst competitor. Similarly, competitive reversals occur if either of the consumers has a higher patch preference for the patch where resource is less consumed.

The observed competitive reversals show a mechanism of bottom-up regulation of intraguild predation communities, based on movement behavior of resource population (Holt and Bonsall 2017). This allows us to question if top-down regulations, based on predator patch preference, are possible in apparent competition interactions. Consider an invasive generalist predator that induces apparent competition between species of the resident community. In homogeneous landscapes, we expect the classical results of Holt (1977), where prey species coexist at lower densities or that one excludes the other. In heterogeneous landscapes, however, consumer patch preference may shift expected exclusion regimes into coexistence ones and vice-versa, while also shifting exclusion of one prey species to the other. This can be possibly verified in a similar framework as displayed here, following Ovaskainen and Cornell (2003); Maciel and Lutscher (2013) to describe species behavior at patch interface and Yurk and Cobbold (2018); Cobbold et al. (2022) to obtain approximate results, highlighting possible future venues where this framework can be applied.

Our work shows that a landscape composed by different patch types with similar lengths/areas, where species can interact and live, can be either detrimental or beneficial for biodiversity in intraguild predation communities and has several implications in the context of biological invasions or reintroduction. By mutual invasion facilitation, we have possible coexistence regimes which would be otherwise unattainable. For hindered mutual invasion conditions, expected coexistence regimes might collapse, and IG predator may become dominant even if IG prey is the best competitor and carrying capacities are adequate in each of the patch types isolated.

Acknowledgements We would like to thank Frithjof Lutscher, who SP discussed the work with on some occasions and provided advice and critique on analysis and recommended some references. We would also like to thank the reviewer and editor for their comments.

Author Contributions SP wrote the first draft, conducted numerical analysis, and produced the figures in the text. SP, RAK, and RMC envisioned the study, reviewed and edited the first draft, leading to the final manuscript.

Funding The authors were funded by different institutions. SP was funded by FAPESP (18/24037-4) and RAK by FAPESP (2021/14335-0) and CNPq (315641/2021-5).

Data availability No datasets were generated or analyzed during the current study.

Declarations

Conflict of Interest The authors declare no competing interests.

References

Abrams PA (2007) Habitat choice in predator-prey systems: spatial instability due to interacting adaptive movements. Am Nat 169(5):581–594

Alhmedi A, Haubruge Francis F (2010) Intraguild interactions implicating invasive species: Harmonia axyridis as a model species. Biotechnol Agron Soc Environ

Armstrong RA, McGehee R (1980) Competitive exclusion. Am Nat 115(2):151–170. Publisher: [University of Chicago Press, American Society of Naturalists]. Accessed 2023-08-20

Amarasekare P (2007) Spatial dynamics of communities with intraguild predation: the role of dispersal strategies. Am Nat 170(6):819–831

Bampfylde C, Lewis M (2007) Biological control through intraguild predation: case studies in pest control, invasive species and range expansion. Bull Math Biol 69:1031–1066

Cantrell RS, Cosner C, Fagan WF (1998) Competitive reversals inside ecological reserves: the role of external habitat degradation. J Math Biol 37(6):491–533. https://doi.org/10.1007/s002850050139. Accessed 2023-08-22

Castillo-Chavez C, Li B, Wang H (2013) Some recent developments on linear determinacy. Math Biosci Eng 10(5&6):1419–1436

Cobbold CA, Lutscher F, Yurk B (2022) Bridging the scale gap: predicting large-scale population dynamics from small-scale variation in strongly heterogeneous landscapes. Methods Ecol Evol 13(4):866–879

Fisher RA (1937) The wave of advance of advantageous genes. Ann eugenics 7(4):355–369

Fritts TH, Rodda GH (1998) The role of introduced species in the degradation of island ecosystems: a case history of Guam. Ann Rev Ecol Syst 29(1):113–140. https://doi.org/10.1146/annurev.ecolsys.29.1.113. Accessed 20 Aug 2023

Grosholz ED, Ruiz GM (1995) Spread and potential impact of the recently introduced European green crab, Carcinus maenas, in central California. Marine Biol 122(2):239–247. https://doi.org/10.1007/BF00348936. Accessed 20 Aug 2023

Hall RJ (2010) Eating the competition speeds up invasions. Biol Lett 7(2):307–311. https://doi.org/10.1098/rsbl.2010.0766. Publisher: Royal Society. Accessed 27 Feb 2024

Holt RD, Bonsall MB (2017) Apparent competition. Ann Rev Ecol Evol Syst 48(1):447–471. https://doi.org/10.1146/annurev-ecolsys-110316-022628. Accessed 22 Aug 2023

Holling CS (1959) Some characteristics of simple types of predation and parasitism. Can Entomol 91(7):385–398. https://doi.org/10.4039/Ent91385-7. Publisher: Cambridge University Press. Accessed 19 June 2023

Holt RD (1997) Predation, apparent competition, and the structure of prey communities. Theor Popul Biol 12(2):197–229. https://doi.org/10.1016/0040-5809(77)90042-9. Accessed 17 Aug 2023

Hosono Y (1998) The minimal speed of traveling fronts for a diffusive Lotka-Volterra competition model. Bull Math Biol 60(3):435–448. https://doi.org/10.1006/bulm.1997.0008. Accessed 19 June 2023

Holt RD, Polis GA (1997) A theoretical framework for intraguild predation. Am Nat 149(4):745–764

Kolmogorov A,Piscounoff N, Petrovsky I (1937) Etude de l'equation de la diffusion avec croissance de la quantite de matiere et son application a un probleme biologique. Moscow Univ Bull Math 1:1–25. Accessed 08 May 2023

Klausmeier CA, Tilman D (2002) Spatial models of competition. In: Sommer U, Worm B (eds) Competition and Coexistence, pp 43–78. Springer, Berlin, Heidelberg. https://doi.org/10.1007/978-3-642-56166-5_3

Lewis MA, Li B, Weinberger HF (2002) Spreading speed and linear determinacy for two-species competition models. J Math Biol 45(3):219–233. https://doi.org/10.1007/s002850200144. Accessed 29 June 2023

Lewis MA, Petrovskii SV, Potts JR (2016) The mathematics behind biological invasions. https://link.springer.com/book/10.1007/978-3-319-32043-4. Accessed 06 May 2024

Malchow H (1997) Spatio-temporal pattern formation in nonlinear non-equilibrium plankton dynamics. Proceedings of the Royal Society of London. Ser B Biol Sci 251(1331):103–109. https://doi.org/10.1098/rspb.1993.0015. Publisher: Royal Society. Accessed 21 Aug 2023

Maciel G, Cosner C, Cantrell RS, Lutscher F (2018) Evolutionarily stable movement strategies in reaction–diffusion models with edge behavior. J Math Biol 1–32

Maciel GA, Lutscher F (2013) How individual movement response to habitat edges affects population persistence and spatial spread. Am Nat 182(1):42–52

Maciel GA, Lutscher F (2018) Movement behaviour determines competitive outcome and spread rates in strongly heterogeneous landscapes. Theor Ecol 11:351–365

Montserrat M, MagalhãesS Sabelis MW, Roos AM, Janssen A (2012) Invasion success in communities with reciprocal intraguild predation depends on the stage structure of the resident population. Oikos 121(1):67–76. https://doi.org/10.1111/j.1600-0706.2011.19369.x. Accessed 20 Aug 2023

Malchow H, Petrovskii SV (2002) Dynamical stabilization of an unstable equilibrium in chemical and biological systems. Math Comput Model 36(3):307–319. https://doi.org/10.1016/S0895-7177(02)00127-9. Accessed 10 May 2023

Ovaskainen O, Cornell SJ (2003) Biased movement at a boundary and conditional occupancy times for diffusion processes. J Appl Probab 40(3):557–580

Owen M, Lewis M (2001) How predation can slow, stop or reverse a prey invasion. Bull Math Biol 63(4):655–684

Polis GA, Anderson WB, Holt RD (1997) Toward an integration of landscape and food web ecology: the dynamics of spatially subsidized food webs. Ann Rev Ecol Syst 28(1):289–316. https://doi.org/10.1146/annurev.ecolsys.28.1.289. Accessed 20 Aug 2023

Polis GA, Holt RD (1992) Intraguild predation: the dynamics of complex trophic interactions. Trends Ecol Evol 7(5):151–154. https://doi.org/10.1016/0169-5347(92)90208-S. Accessed 19 Aug 2023

Petrovskii SV, Malchow H (1999) A minimal model of pattern formation in a prey-predator system. Math Comput Model 29(8):49–63. https://doi.org/10.1016/S0895-7177(99)00070-9. Accessed 21 Aug 2023

Petrovskii SV, Malchow H (2000) Critical phenomena in plankton communities: KISS model revisited. Nonlinear Anal Real World Appl 1(1):37–51. https://doi.org/10.1016/S0362-546X(99)00392-2. Accessed 11 May 2023

Polis GA, Myers CA, Holt RD (1989) The ecology and evolution of intraguild predation: potential competitors that eat each other. Ann Rev Ecol Syst 20(1):297–330. https://doi.org/10.1146/annurev.es.20.110189.001501. Accessed 19 Aug 2023

Schtickzelle N, Baguette M (2003) Behavioural responses to habitat patch boundaries restrict dispersal and generate emigration–patch area relationships in fragmented landscapes. J Anim Ecol 72(4):533–545. https://doi.org/10.1046/j.1365-2656.2003.00723.x. Accessed 18 Aug 2023

Skellam JG (1951) Random dispersal in theoretical populations. Biometrika 38(1–2):196–218. https://doi.org/10.1093/biomet/38.1-2.196. Accessed 08 May 2023

Shigesada N, Kawasaki K, Teramoto E (1986) Traveling periodic waves in heterogeneous environments. Theor Popul Biol 30(1):143–160

Tuckett QM, Deacon AE, Fraser D, Lyons TJ, Lawson K, Hill JE (2021) Unstable intraguild predation causes establishment failure of a globally invasive species. Ecol 102(8):03411. https://doi.org/10.1002/ecy.3411. Accessed 29 Feb 2024

Tilman D et al (1990) Mechanisms of plant competition for nutrients: the elements of a predictive theory of competition. Mechanisms of plant competition for nutrients: the elements of a predictive theory of competition. 117–141

Weinberger HF (1978) Asymptotic behavior of a model in population genetics. In: Chadam JM (ed) Nonlinear Partial Differential Equations and Applications. Lecture Notes in Mathematics, pp 47–96. Springer, Berlin, Heidelberg. https://doi.org/10.1007/BFb0066406

Weinberger HF (1982) Long-time behavior of a class of biological models. SIAM J Math Anal 13(3):353–396

Yurk BP, Cobbold CA (2018) Homogenization techniques for population dynamics in strongly heterogeneous landscapes. J Biol Dynamics 12(1):171–193